SAND 99-1053J

In-Situ Monitoring of GaSb, GaInAsSb, and AlGaAsSb*

C.J. Vineis[1,2,†], C.A.Wang[1], K.F. Jensen[2,3], and W.G. Breiland[4]
[1]Lincoln Laboratory, Massachusetts Institute of Technology, Lexington, MA 02173-9108
[2]Dept. of Materials Science and Engineering, Massachusetts Institute of Technology, Cambridge, MA 02139-4307
[3]Dept. of Chemical Engineering, Massachusetts Institute of Technology, Cambridge, MA 02139-4307
[4]Sandia National Laboratories, Albuquerque, New Mexico 87185-0601

Abstract

The suitability of the wavelength range provided by silicon photodiode detector arrays for monitoring the spectral reflectance during epitaxial growth of GaSb, AlGaAsSb, and GaInAsSb, which have cutoff wavelengths at 25°C of 1.7, 1.2, and 2.3 μm, respectively, is demonstrated. These alloys were grown lattice matched to GaSb in a vertical rotating-disk reactor, which was modified to accommodate near normal reflectance without affecting epilayer uniformity. By using a virtual interface model, the growth rate and complex refractive index at the growth temperature are extracted for these alloys over the 600 to 1000 nm spectral range. Excellent agreement is obtained between the extracted growth rate and that determined by ex-situ measurement.

KEYWORDS: GaInAsSb, AlGaAsSb, GaSb, in situ reflectance monitoring, organometallic vapor phase epitaxy, OMVPE

PACS: 81.15.Kk (Vapor phase epitaxy)

Sandia is a multiprogram laboratory operated by Sandia Corporation, a Lockheed Martin Company, for the United States Department of Energy under contract DE-AC04-94AL85000.

*This work was sponsored by the Department of Energy under AF Contract No. F19628-95-C-0002. The opinions, interpretations, conclusions and recommendations are those of the author and are not necessarily endorsed by the United States Air Force.

† email: cjv@ll.mit.edu

1. Introduction

In-situ optical monitoring during organometallic vapor phase epitaxy (OMVPE) provides insight into complex growth processes, and has led to improvements in the growth process and the resulting materials. Techniques for monitoring the epitaxial growth include spectral reflectance (SR), thermal emission, spectroscopic ellipsometry (SE), reflectance difference spectroscopy (RDS), and surface photoabsorption (SPA) [1]. Each of these optical probes is sensitive to different properties of a material, and thus could be used simultaneously to obtain complementary information during epitaxial growth. For example, RDS has been demonstrated to be a useful method for monitoring surface processes [2], while SE enables accurate determination of thin film refractive indices and thicknesses [3]. SR can yield real-time information on the growth rate and complex refractive index [4-10], or more qualitative information such as "fingerprints" of growth runs [11-13].

Near-normal SR is a particularly attractive technique for in-situ monitoring because it provides information that can be quickly analyzed for closed-loop process control [5], and is less expensive and easier to implement than most other in-situ process monitors. In previous studies, Si detectors were used. However, since antimonide-based alloys have smaller bandgaps and higher absorption over the Si wavelength range (typically 400-1100 nm), it is not apparent whether these alloys are transparent enough in the Si detector wavelength range to enable growth rate and optical constant determination from the classical Fabry-Perot interference oscillations. Previous work in InP-based materials indicated that absorption was significant in the wavelength range of the silicon detector, and improved results were obtained by using a PbS detector to extend the wavelength range to 2500 nm [7,8].

DISCLAIMER

Since it is desirable to use off-the-shelf, readily available components to maintain low costs, we investigated the usefulness of a conventional Si photodiode array (PDA) for monitoring in-situ the SR during growth of III-V antimonide-based materials. In this paper, we demonstrate that a Si PDA provides sufficient SR for determination of growth rates and optical constants of GaSb, AlGaAsSb, and GaInAsSb. Extracted growth rates compare favorably with layer thicknesses determined ex-situ using high resolution x-ray diffraction (HRXRD).

2. Experimental procedure and reactor development

Figure 1 shows a schematic diagram of the experimental setup. Optical fibers are used to direct white light from a 5 W tungsten halogen lamp to the vertical rotating-disk reactor, and the reflected signal to the Si PDA spectrometer, which interfaces directly to the computer. The Si spectrometer is a commercial 512 element array with a dispersive element and has a wavelength range of 380 to 1100 nm with a 1.3 nm spectral resolution. Integration times as low as 10 ms may be used to acquire spectra, although for our growth rates a one second integration time was sufficient. The unit is compact and entirely contained on a PC card that plugs directly into a computer expansion slot. Calibration of the spectrometer to provide absolute reflectance values was accomplished by referencing the raw counts of a silver mirror to the mirror's absolute spectral reflectance. The SR as a function of growth time was acquired via a Windows-based program and stored to disk. Quantitative analysis of the reflectance was performed using a virtual interface (VI) model [4] to yield the growth rate and complex refractive index.

The vertical rotating-disk reactor utilizes a mesh screen to ensure plug flow into the reactor [14], and was modified to incorporate an optical window at the center of the mesh. The diameter of the optical window is constrained by epitaxial growth nonuniformities and heterostructure grading that could occur if the unswept volume below the window is too large. In order to assess the effects of window diameter on growth, numerical simulations (similar to those of ref. 15) of the flow and temperature fields were performed for the reactor under typical growth conditions: 10-cm-diam quartz tube, 15 cm inlet-to-susceptor distance, 10 slpm H_2 carrier flow rate, 150 Torr reactor pressure, 550°C susceptor temperature, and 400 rpm susceptor rotation rate. The window radius was either 1.27 or 2.54 cm. For the 1.27-cm-radius window, shown in Fig. 2a, the gas sweeps out the volume below the window with minimal change in temperature and flow fields compared to those computed without the window [14]. Consequently, the epitaxial growth characteristics are preserved. When the window radius is increased to 2.54 cm, shown in Fig. 2b, gas expansion results in a recirculation below the window which can lead to heterostructures with graded interfaces. Because of high gas diffusivity, layer uniformity is unaffected by the larger optical window. The total obstruction from the optical window and mounting flanges used in these experiments has a 1.9 cm radius.

GaSb, $Ga_{0.83}In_{0.17}As_{0.16}Sb_{0.84}$, and $Al_{0.2}Ga_{0.8}As_{0.02}Sb_{0.98}$ epilayers with 25°C cutoff wavelength, λ, ~ 1.7, 2.3, and 1.2 μm, respectively, were grown lattice matched to GaSb in the vertical rotating-disk reactor with H_2 carrier gas at a flow rate of 10 slpm and reactor pressure of 150 Torr, as described previously [16]. Triethylgallium, trimethylindium, tritertiarybutylaluminum, trimethylantimony, and tertiarybutylarsine were used as precursors. Layers were grown at 525 or 550°C on Te-doped GaSb, (100) misoriented 6° toward (111)B. Epilayer composition was determined from HRXRD splitting of ω-2Θ scans, the peak emission in 300 K photoluminescence spectra, and the energy gap dependence on composition. Epitaxial layer thickness was determined within ± 5% by HRXRD, using software based on the Taupin-Tagachi solution to dynamical x-ray diffraction.

3. Results and discussion

Reflectance at 650, 800, and 1000 nm as a function of time is shown in Fig. 3. The initial 600 s corresponds to heat-up of the GaSb substrate from 25 to 525°C (Figs. 3a and 3c), or to 550°C (Fig. 3b). It is evident from Figs. 3a and 3c that the reflectance signal during heat-up is consistent. A slight drop in reflectance is observed at all wavelengths at 250 s, which corresponds to a temperature of 480°C. This drop might be associated with oxide lift-off, causing the surface to roughen. Similar observations by SPA have been reported [17].

The heat-up period is followed by 200 s growth of GaInAsSb (Fig. 3a), 1000 s of AlGaAsSb growth (Fig. 3b), or 42 s of GaInAsSb spacer layer growth and 1500 s of GaSb growth (only the initial 1360 s of GaSb layer growth are shown, Fig. 3c). The GaInAsSb spacer layer is necessary to obtain oscillations from GaSb growth on a GaSb substrate.

In all cases a small amplitude, high frequency signal is superimposed on the main signal related to layer growth. This high frequency signal is a beat frequency which arises due to susceptor wobble during rotation, and imperfect synchronization between the data acquisition and susceptor rotation rates. The effect of susceptor wobble has only a slight influence on data accuracy as discussed below.

Quantitative analysis of the reflectance to extract growth rates and optical constants requires a minimum degree of transparency of a growing layer. Ideally, at least one full oscillation period should exist for the most accurate curve fitting analysis [4]. However, because absorption becomes significant for wavelengths much smaller than the bandgap of the layer, the oscillation amplitude decreases with increasing growth time. Figure 3 shows that for wavelengths longer than 800 nm, at least one oscillation occurs before the onset of significant absorption in all three materials, indicating that the wavelength range of Si photodiode arrays is suitable for monitoring the growth of these III-V antimonides.

Using a VI model [4], the growth rates of GaInAsSb at 525°C, AlGaAsSb at 550°C, and GaSb at 525°C were extracted at several wavelengths between 650 and 1000 nm from the data shown in Fig. 3. Accurate curve fitting at wavelengths shorter than 750 nm was not possible for the GaInAsSb layer for two reasons. First, high absorption in the GaInAsSb layer limited the number of Fabry-Perot oscillations. Second, the GaInAsSb alloy composition was such that its complex refractive index, N, is similar to the GaSb substrate ($N_{GaInAsSb}$=4.73-i*0.73 vs. N_{GaSb}=4.97-i*0.65, at 800 nm and 525°C [results from this work]), resulting in oscillations with small amplitudes (see Fig. 3a). Therefore, the noise due to susceptor wobble places limitations on the signal-to-noise ratio. Wavelengths below 750 nm gave erroneously low growth rate values. Extracted growth rates from wavelengths between 750 nm and 1000 nm, however, were consistent to within 0.4%. Therefore, reflectance signals at the longer wavelengths were used for more accurate data analysis. Analysis of the AlGaAsSb and GaSb layers indicated that wavelengths as short as 650 nm were still acceptable for extracting growth rates.

Film thicknesses determined from the in-situ reflectance are 234.0 nm ± 10.0 nm for the GaInAsSb layer, 273.0 nm ± 11.0 nm for the AlGaAsSb layer, and 360.0 nm ± 14.4 nm for the GaSb layer. These values agree well with thicknesses determined ex-situ by HRXRD: 231.0 nm ± 11.6 nm for the GaInAsSb layer, 263.2 nm ± 13.2 nm for the AlGaAsSb layer, and 369.5 nm ± 18.5 nm for the GaSb layer. Error in growth rate determination from the in-situ reflectance is directly related to the ability of the reflectance set-up to accurately measure absolute reflectance values. Knowledge of the absolute reflectance, and not simply the relative reflectance, is necessary for the virtual interface model to correctly separate the real part of the refractive index, n, from the growth rate, G, yielding physical growth rates (G) instead of optical thickness growth rates (n*G) [4].

The growth of a GaSb epilayer at 550°C on a GaSb substrate was also monitored, yielding an in-situ thickness determination of 417.0 nm ± 16.7 nm. Ex-situ HRXRD measurements determined an actual film thickness of 431.7 nm ± 21.6 nm. Comparison of this layer with the GaSb grown at 525°C above therefore indicates an increase of the GaSb growth rate from 0.240 nm/s to 0.278 nm/s upon increasing the growth temperature from 525 to 550°C.

Optical constants (n and k) at the growth temperature for all three layers were also extracted using the VI model, and are shown in Fig. 4 for GaInAsSb at 525°C, AlGaAsSb at 550°C, and GaSb at 550°C. The accuracy of these values is limited by the accuracy of the absolute reflectance values determined by the reflectance set-up, which have been determined to be ±4% for our system. Unfortunately, little information is available about the refractive indices of these materials at the elevated growth temperatures. Therefore, comparison of our extracted data to literature values is not possible.

4. Summary

Near-normal SR using a Si photodiode array has been demonstrated as a useful tool for monitoring the growth of III-V antimonide-based alloys. Growth rates extracted from the reflectance signal at wavelengths longer than 750 nm compare favorably with film thicknesses measured ex-situ using HRXRD. Optical constants at growth temperatures have also been extracted from the reflectance for GaSb, AlGaAsSb, and GaInAsSb.

Acknowledgments

The authors gratefully acknowledge S.R. Chinn and D.L. Spears for helpful discussions; T.G. Mihopoulos for finite element calculations; D.C. Oakley, J.W. Chludzinski, and J.W. Caunt for assistance in experimental design and crystal growth; and D.R. Calawa for x-ray diffraction.

References

1. I. P. Herman, *Optical Diagnostics for Thin Film Processing*. Academic Press, New York, 1996.

2. D.E. Aspnes, IEEE J. Quantum Electron. 25 (1989) 1056.

3. E. A. Irene, Thin Solid Films 233 (1993) 96.

4. W. G. Breiland and K. P. Killeen, J. Appl. Phys. 78 (1995) 6726.

5. H. Sankur, W. Southwell, and R. Hall, J. Electron. Mater. 20 (1991) 1099.

6. N.C. Frateschi, S.G. Hummel, and P.D. Dapkus, Electron. Lett. 27 (1991) 155.

7. J. C. Bean, L. J. Peticolas, R. Lum, and M. L. McDonald, J. Vac. Sci. Technol. A 14 (1996) 946.

8. R. M. Lum, M. L. McDonald, J.C. Bean, J. Vandenberg, T. L. Pernell, S. N. G. Chu, A. Robertson, and A. Karp, Appl. Phys. Lett. 69 (1996) 928.

9. T. Farrell, J.V. Armstrong, and P. Kightley, Appl. Phys. Lett. 59 (1991) 1203.

10. J. Bajaj, S.J.C. Irvine, and H.O. Sankur, J. Electron. Mater. 22 (1993) 899.

11. K. Killeen, M.J. Ludowise, W.H. Perez, S.D. Lester, Y-L. Chang, D. Lefforge, and J.N. Miller, 8th Biennial Workshop on Organometallic Vapor Phase Epitaxy, April 1997, Dana Point, CA.

12. K.P. Killeen and W.G. Breiland, J. Electron. Mater. 23 (1994) 179.

13. R.M. Biefeld, A.A. Allerman, S.R. Kurtz, and K.C. Baucom, Proc. ICMOVPE IX, La Jolla, CA 1998.

14. C.A. Wang, S. Patnaik, J.W. Caunt, and R.A. Brown, J. Cryst. Growth 93 (1988) 228.

15. T.G. Mihopoulos, Ph.D. thesis, Massachusetts Institute of Technology, 1998.

16. C.A. Wang, accepted J. Cryst. Growth.

17. N.J Mason and P.J. Walker, Proc. ICMOVPE IX, La Jolla, CA 1998.

Figure Captions

Figure 1. Schematic diagram of the experimental setup for in-situ process monitoring using near-normal spectral reflectance.

Figure 2. Simulated flow patterns in the reactor under typical growth conditions, calculated using finite element analysis. Comparison is made between a window radius of: (a) 1.27 cm and (b) 2.54 cm. Note the recirculating flow immediately under the window in (b).

Figure. 3. Reflectance as a function of time at 650, 800, and 1000 nm, for the heat-up of a GaSb substrate (600 s), followed by: (a) growth of a lattice matched GaInAsSb layer at 525°C; (b) growth of a lattice matched AlGaAsSb layer at 550°C, or; (c) growth of a thin lattice matched GaInAsSb spacer layer and thick GaSb layer at 525°C. Data are displayed on the same scale to compare the run-to-run heat-up similarity.

Figure 4. Complex refractive indices of: (a) GaInAsSb ($\lambda \sim 2.3$ μm at 25°C) at 525°C; (b) AlGaAsSb ($\lambda \sim 1.2$ μm at 25°C) at 550°C, and; (c) GaSb at 550°C. Error of extracted n and k values is $\pm 4\%$, due to error in accurately determining the absolute reflectance.

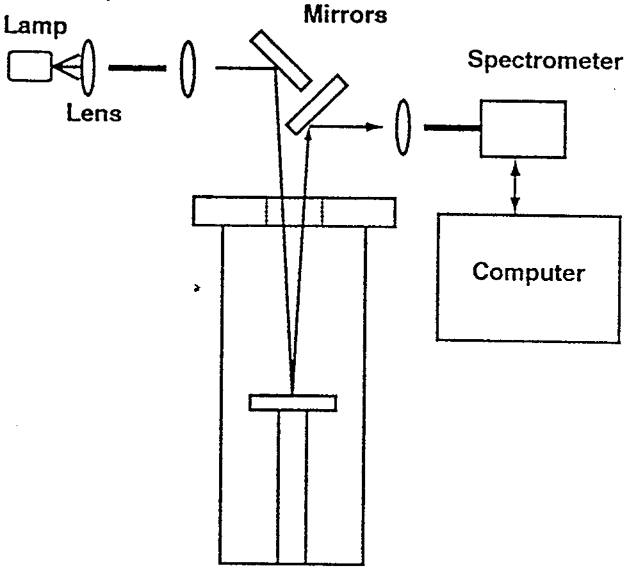

Vertical Rotating Disk Reactor

Figure 1

317395-1

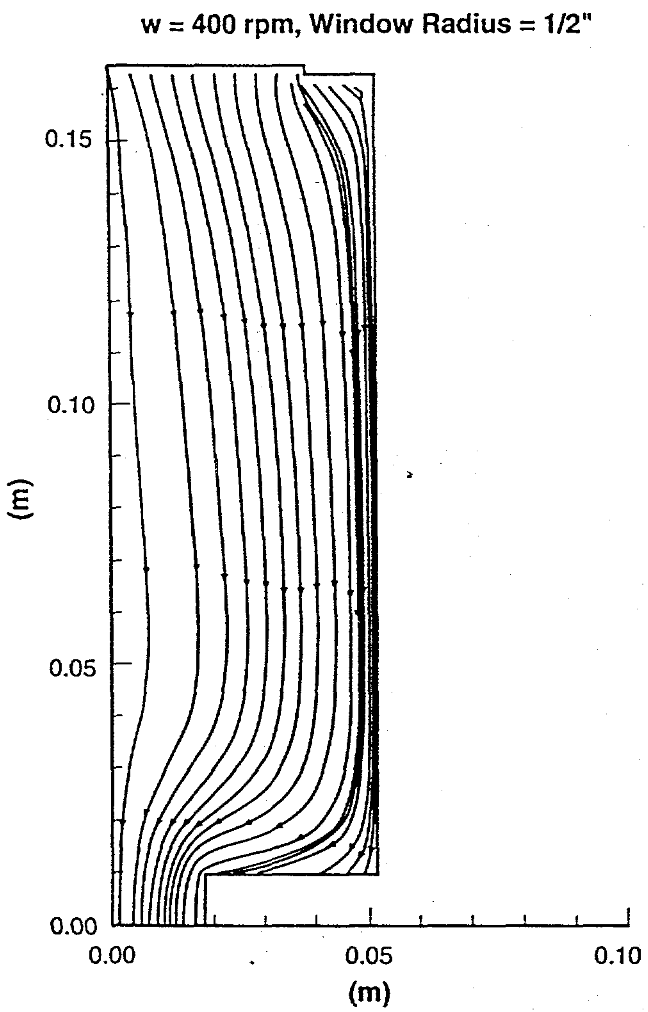

Figure 2a

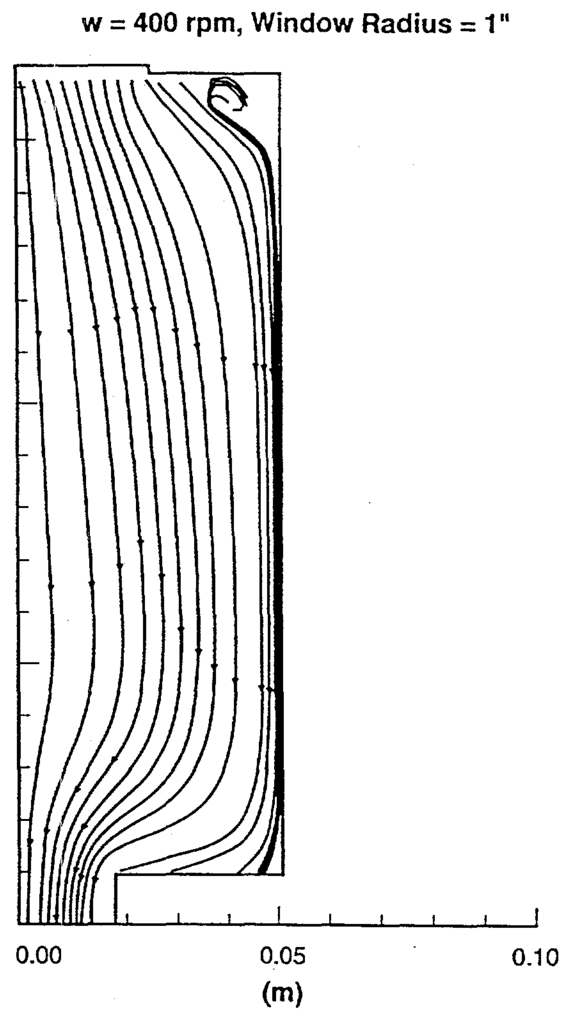

Figure 2b

317395-4B

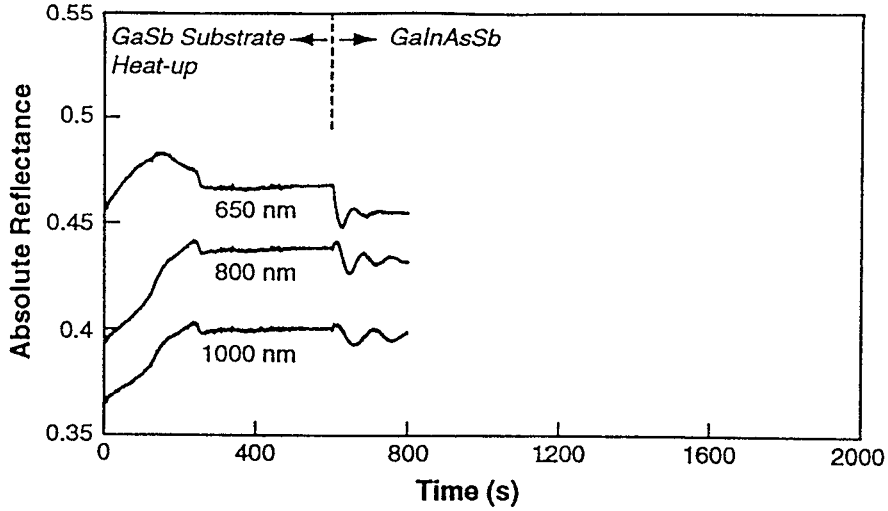

Figure 3(a)

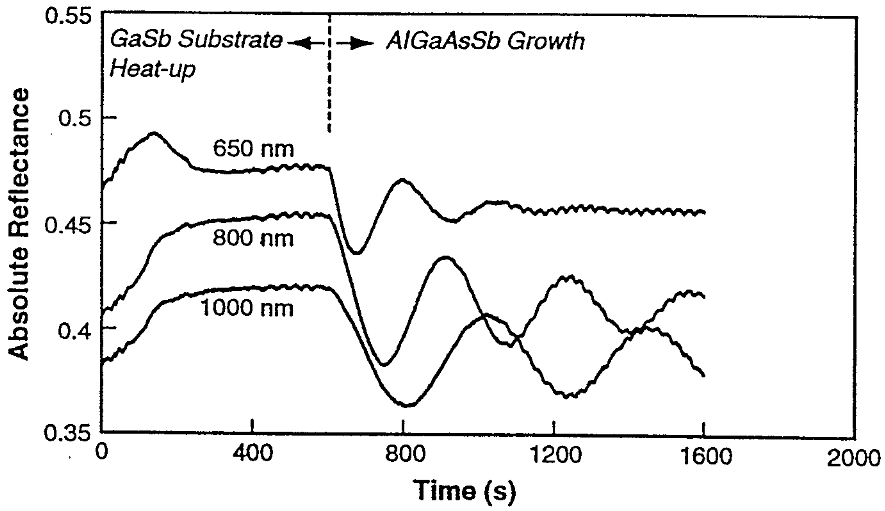

Figure 3(b)

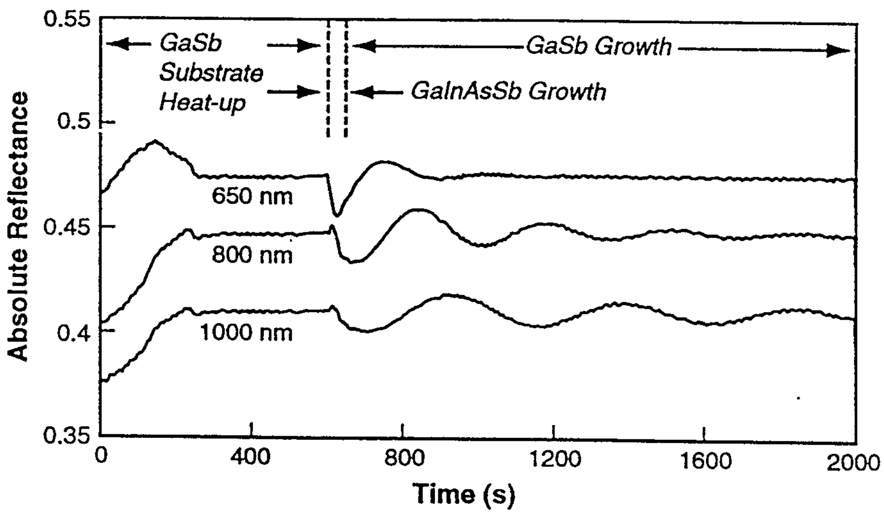

Figure 3(c)

317395-2

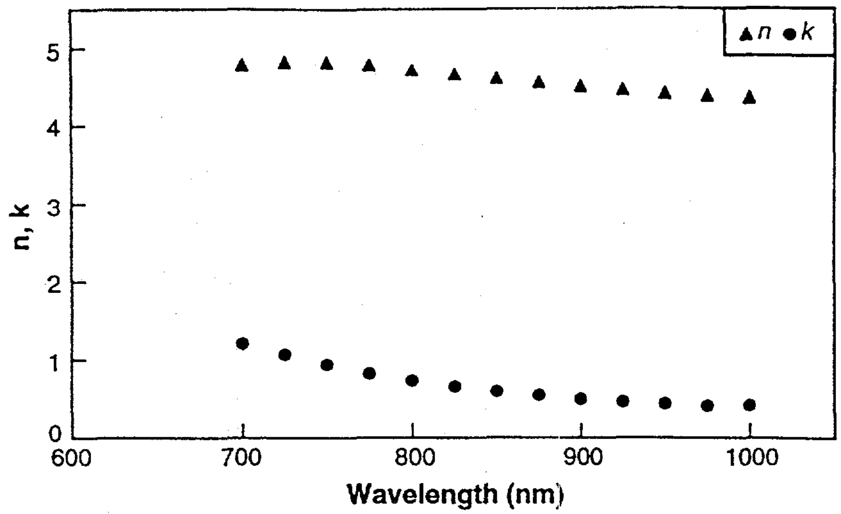

Figure 4(a)

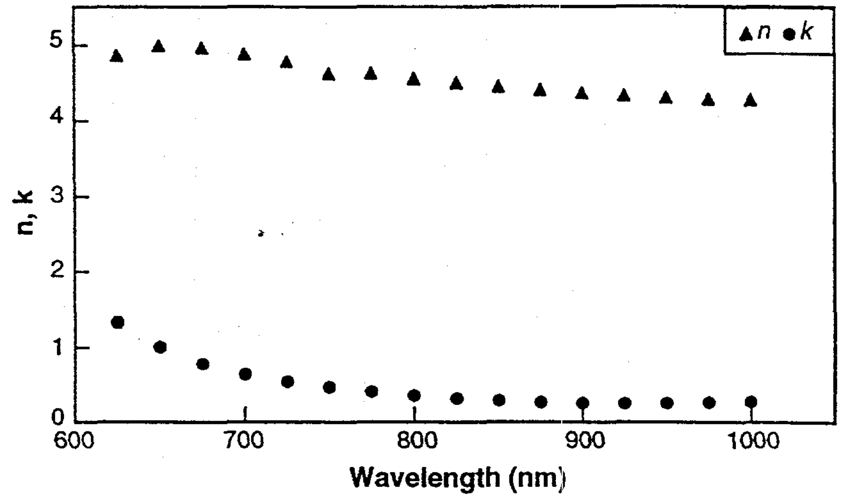

Figure 4(b)

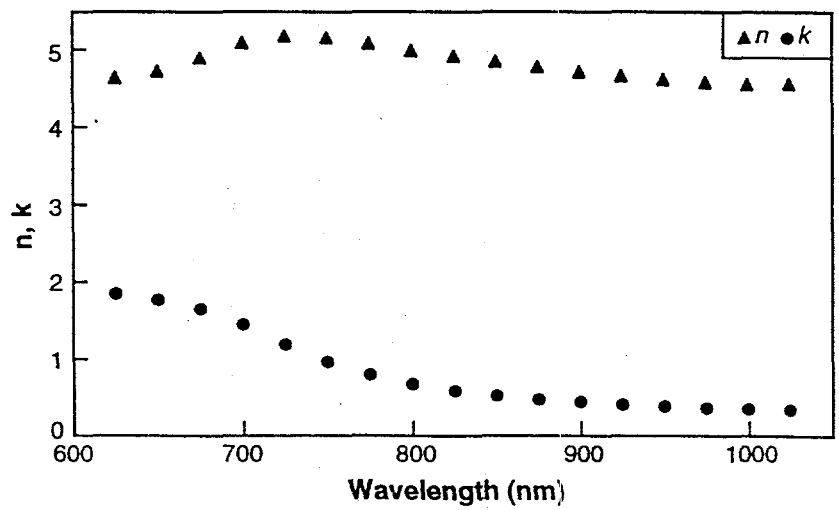

Figure 4(c)

317395-3